STUDIA UBB CHEMIA, LXI, 4, 2016 (p. 177 - 188)
(RECOMMENDED CITATION)

BEHAVIOUR OF TWELVE SPHERICAL CODES IN CW EPR POWDER SIMULATIONS. UNIFORMITY AND EPR PROPERTIES

CORA CRĂCIUN[a]*

ABSTRACT. This paper assesses the efficiency of twelve spherical codes in CW EPR powder simulations. The spherical codes are either regular or are generated using optimisation methods. The EPR simulations are performed for spin systems with axial and rhombic symmetry. The spherical codes are compared using Voronoi tessellation-based homogeneity and EPR properties.

Keywords: *CW EPR powder simulations, spherical code, uniformity degree, EPR metrics*

INTRODUCTION

Continuous-wave electron paramagnetic resonance (CW EPR) powder simulations use spherical sets of points to approximate numerically the EPR spectrum. The quality of the EPR simulations depends both on the spherical codes' properties (size, uniformity degree) and the EPR characteristics of the spin system investigated (spin state, symmetry).

Previous assessments of the spherical codes for magnetic resonance simulations were based on the codes' homogeneity [1], the convergence rate of the simulations [2,3], and on EPR metrics [4]. The EPR metrics defined in [4] and some of the homogeneity metrics [4,5] depend on the spherical codes' Voronoi tessellation generated on the unit sphere.

This paper assesses the behaviour in CW EPR powder simulations and computes some homogeneity and EPR properties for the following spherical codes (the grids' abbreviations used in the paper are given in parentheses): Concentric map (CM) [6,7], HEALPix (HPX) [8,9], Cubed-sphere (CS) [10-13], Minimum Energy (ME) [14-16], Maximum Determinant (MD) [14,15,17], Symmetric Spherical grid (SS) [14,15,18], Icosahedral - covering arrangement (icover) [19],

[a] *Babeş-Bolyai University, Faculty of Physics, 1 Kogălniceanu str., RO-400084 Cluj-Napoca, Romania*
** Corresponding author: cora.craciun@phys.ubbcluj.ro*

Icosahedral - packing arrangement (ipack) [19], Icosahedral - maximal volume arrangement (ivol) [19], Hammersley (Ham) [20-24], Repulsion (Rep) [3,25], and Spherical Centroidal Voronoi Tessellation (SCVT) spherical code [26-29].

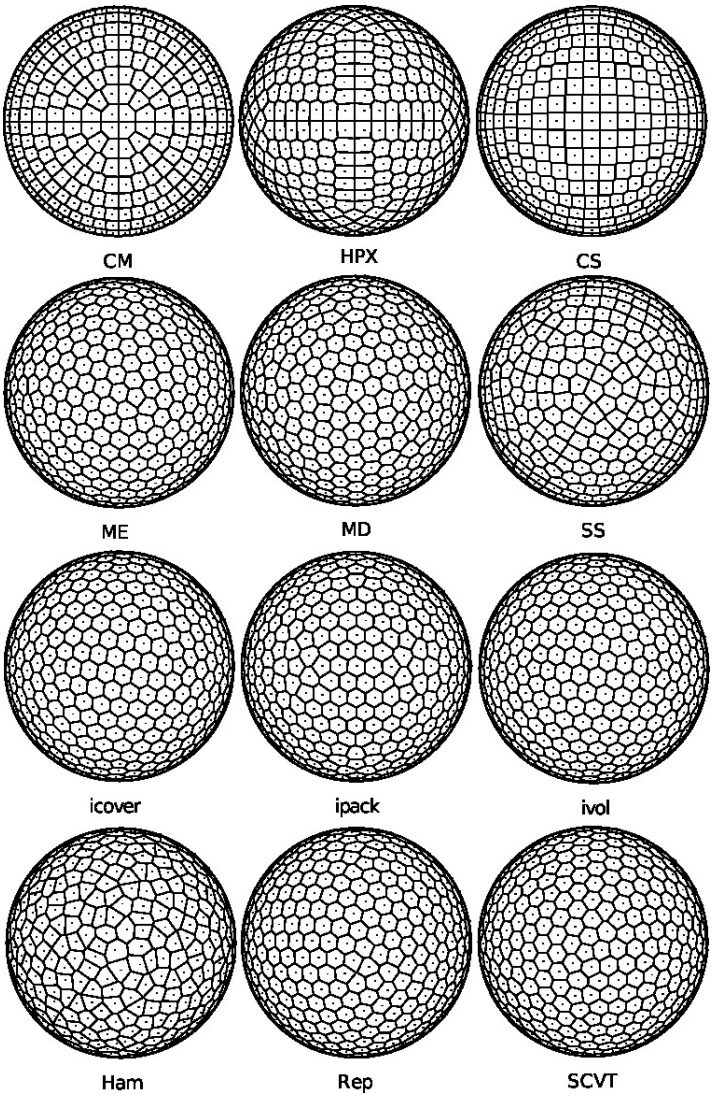

Figure 1. The upper hemisphere and the Voronoi tessellation of the following spherical codes (the full sphere number of points is given in parentheses): CM (580), HPX (588), CS (602), ME (576), MD (576), SS (564), icover (572), ipack (582), ivol (572), Ham (578), Rep (578), and SCVT (578).

(a) *Concentric map* (CM) has been proposed for ray tracing applications in computer graphics, in order to maintain the adjacency and relative proportions when mapping patches from one surface to another [6,7]. First, CM maps square grids on disks, by transforming concentric squares of points into concentric circles of points [7]. Then, the points on the disk are uniformly projected onto the upper hemisphere [7]. The points on the lower hemisphere are obtained by mirror symmetry with respect to the xOy plane.

(b) *HEALPix* (Hierarchical Equal Area isoLatitude Pixelization) was developed for astronomy applications involving fast processing of functions, such as spherical harmonic transforms, on spherical regions [8,9]. The HEALPix tessellation partitions the sphere in quadrilateral regions of equal areas, called pixels. The pixel centres (the grid nodes) are equally spaced on curves of constant latitude [8].

(c) The original *Cubed-sphere* grid was introduced by Sadourny, in order to avoid the pole problems in the context of atmospheric motion numerical modelling [10]. The grid is obtained by projecting the six faces of a cube onto the circumscribed sphere. Different projection methods have been proposed, including the gnomonic [11] and conformal [12] mappings. This paper uses the gnomonic equiangular central projection, which yields a non-orthogonal cubed-sphere grid with higher uniformity than other projections [13].

(d-f) The *Minimum Energy*, *Maximum Determinant*, and *Symmetric Spherical* grids were computed by R. S. Womersley and I. H. Sloan for numerical integration on the sphere [14-18]. The Minimum Energy points were obtained by minimizing their Coulomb-type potential energy [14-16]. The Maximum Determinant (Extremal) points were computed by maximizing the determinant of an interpolation matrix, in the space of spherical polynomials [14,15,17]. The Symmetric (antipodal) Spherical code belongs to the category of spherical t-designs, having equal cubature weights for all points [14,15,18].

(g-i) The *Icosahedral* arrangements of points were computed by R. H. Hardin, N. J. A. Sloane, and W. D. Smith [19]. The covering arrangement was obtained by minimizing the covering radius, that is the maximal distance from any point on the sphere to the closest grid point [19]. The packing arrangement was generated by maximizing the minimal distance between the grid points [19]. At its turn, the maximal volume arrangement was computed by maximizing the volume of the points' convex hull [19].

(j) The *Hammersley* spherical code, introduced in [20], is a deterministic low-discrepancy finite point set, based on radical inversion [21]. This point set has proved useful for quasi-Monte Carlo integration [21] and has been used, for example, in various applications in computer graphics [22]. The Hammersley point set on the unit sphere is obtained by projecting a two-dimensional Hammersley set, using a mapping such as Lambert cylindrical equal-area projection [22,23].

(k) The *Repulsion* spherical code has been proposed for Nuclear Magnetic Resonance powder simulations [3,25]. This spherical code is generated iteratively by adjusting the positions of a set of equal electrical charges on the unit sphere. The charges repel each other by Coulomb forces and perform small movements on the sphere until the system reaches equilibrium [25]. At equilibrium, the potential energy of the charge system is minimal.

(l) The *SCVT* grid belongs to the category of energy minimization spherical codes and uses the unit sphere Voronoi tessellation [26-29]. The grid is generated iteratively, the points' positions being adjusted until they coincide with the mass centres (centroids) of their corresponding Voronoi cells [26-29].

The original grids use different tessellations to partition the unit sphere in patches or cells. This paper uses the Voronoi tessellation for all spherical codes, in order to compute the weight corresponding to each grid point in EPR simulations. The Voronoi tessellations of the twelve spherical codes with about 580 points are presented in Figure 1.

RESULTS AND DISCUSSION

1. CW EPR powder simulations

CW EPR powder spectra of the twelve spherical codes have been simulated as described in [4], for a spin system S = 1/2 characterised by electron Zeeman interaction with the static magnetic field. Two different symmetries of the gyromagnetic matrix **g** have been considered: one axial (C3), with the principal values (g_x = 2.0, g_y = 2.0, g_z = 2.2), and one rhombic (C4), with (g_x = 2.0, g_y = 2.1, g_z = 2.2). The two g-cases were denoted as in reference [4], to ease comparison with the results presented there. Pure axial spin systems do not require a spherical code, a quarter of a spherical meridian being sufficient for powder simulations [30]. Nevertheless, the axial case is considered here as an extreme case for nearly axial spin systems. EPR simulations have also been performed for the EasySpin grid [1] with a very high number of points. These simulations illustrate how the experimental spectra would look like for the spin system and symmetries considered in this paper. Based on the EPR simulations (Figures 2 and 3), we make the following observations:

(a) In the *axial case* (C3), the Ham, Rep, ME, MD, ipack, and SCVT spherical codes generate simulated spectra with lower simulation noise than the other spherical codes. However, they do not behave better, for instance, than the Fibonacci grid presented in [4], which yields a nearly noise-free simulated spectrum in the (C3) g-case.

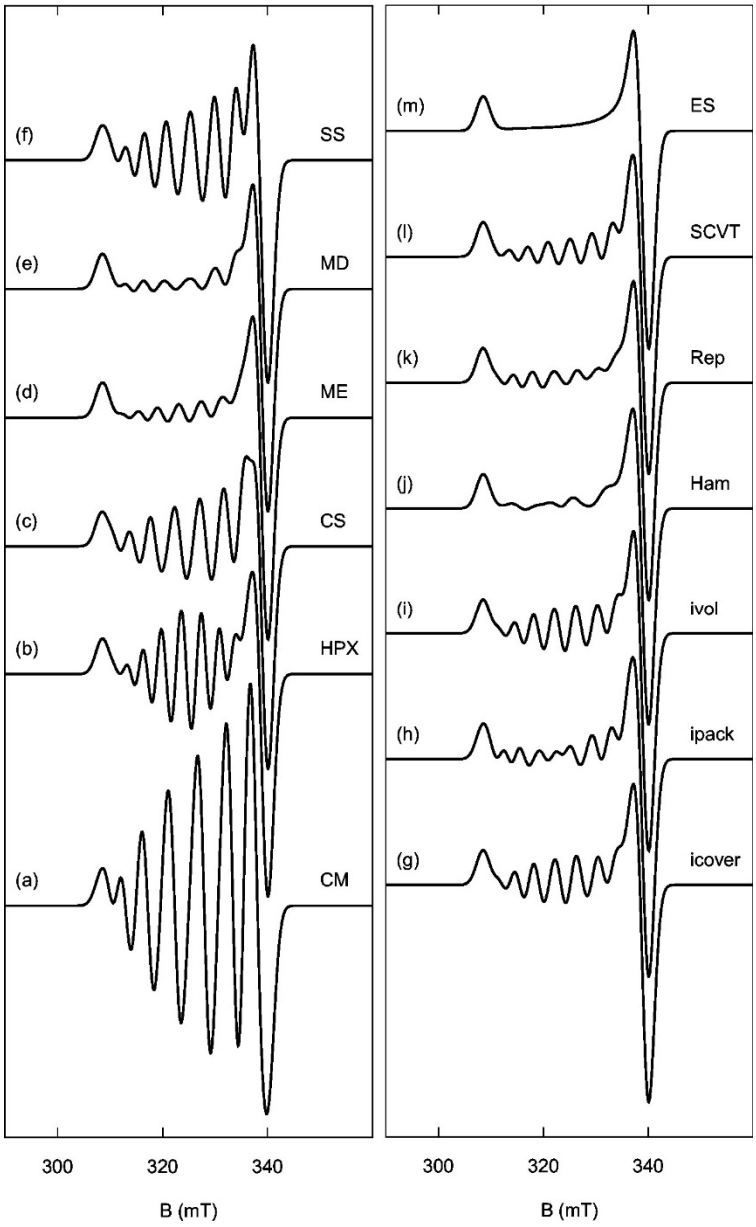

Figure 2. Simulated CW EPR powder spectra for (a-l) the twelve spherical codes with about 580 points and (m) the EasySpin spherical code with 9606 points, in the axial (C3) g-case.

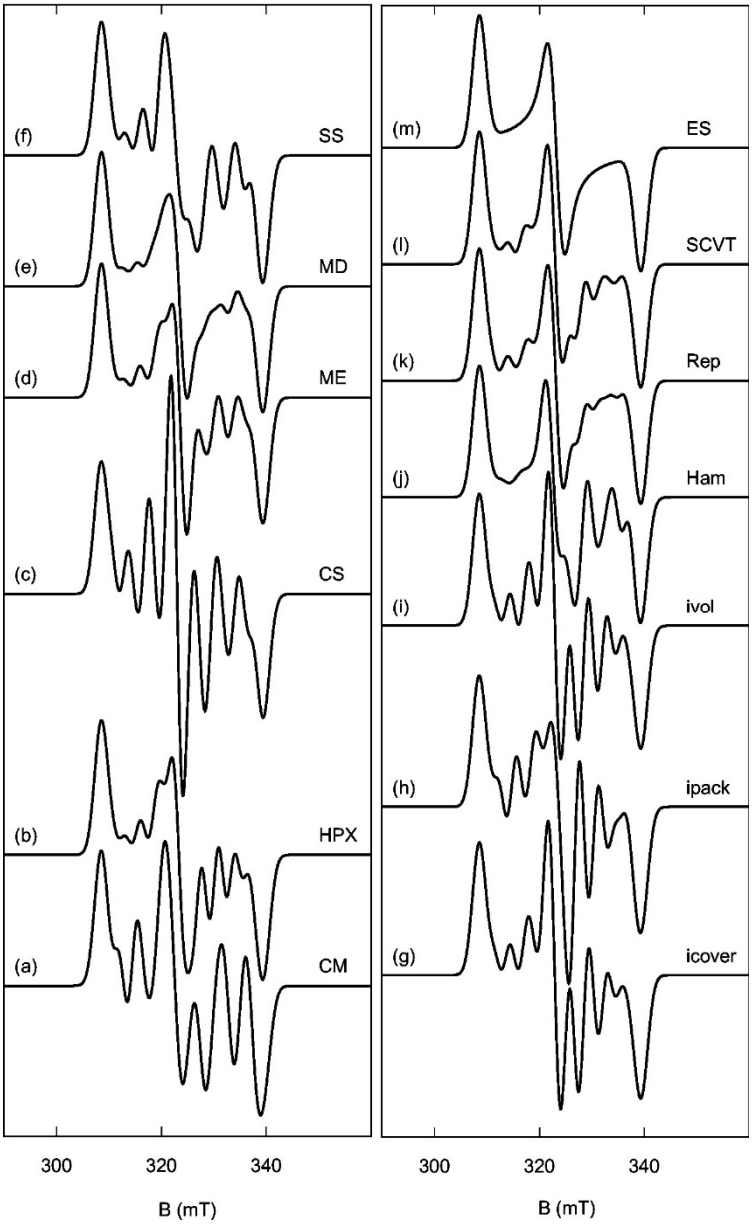

Figure 3. Simulated CW EPR powder spectra for (a-l) the twelve spherical codes with about 580 points and (m) the EasySpin spherical code with 9606 points, in the rhombic (C4) g-case.

(b) In the *rhombic case* (C4), the MD, Rep, and SCVT spherical codes generate less noisy simulated EPR spectra then the other spherical codes. The spectra of these grids have similar quality with the Fibonacci grid's spectrum, but are noisier than the EasySpin grid's spectrum from [4].

2. Homogeneity properties

By Voronoi tessellation, each spherical code generates a structure of Voronoi cells on the unit sphere (Figure 1). If we take the mean distance, $h_{mean}(k)$, between any grid point P_k (k = 1,...,N) and the vertices of its Voronoi cell V_k, we obtain a measure of the grid's homogeneity [4,5].

Figure 4 presents the h_{mean} distributions (the $h_{mean}(k)$ values for all grid points) for the twelve spherical codes discussed in this paper. The icover, ME, and Rep grids, followed by ivol, SCVT, and MD, have the h_{mean} distributions with the smallest spread between the lower and upper whiskers of the boxplot representations. This means that most Voronoi cells of each of these spherical codes are geometrically similar.

3. EPR properties

The two EPR metrics defined in [4] have been calculated for the spherical codes discussed here. The first metric, $B_{dev}(k)$, is the deviation of the resonance magnetic field at the grid point P_k from the mean magnetic field of the corresponding Voronoi cell V_k [4]. The mean field of the Voronoi region is calculated by averaging the resonance magnetic fields at a set of randomly generated points inside this region. The second EPR metric, $B_{ov,max}(k)$, is the maximum overlapping degree between the resonance magnetic field intervals of the Voronoi cell V_k and its adjacent Voronoi cells [4]. This metric quantifies how much the EPR signals generated by adjacent Voronoi regions are overlapping.

The B_{dev} distributions of the grids are presented in Figure 5, for the (C3) and (C4) g-cases. In each case, most spherical codes have similar spread of data, excepting Ham and ipack with the highest range distributions. Compared to the previously investigated EasySpin grid [4], all twelve spherical codes have wider B_{dev} distributions and thus are less EPR homogeneous.

Unlike the B_{dev} metric, $B_{ov,max}$ (Figure 6, Table 1) differentiates better the grids in the axial (C3) g-case. In this case, the CM spherical code presents the highest maximum overlapping degree and behaves as the previously investigated Rectangular grid [4]. In the rhombic (C4) g-case, the twelve spherical codes behave similarly.

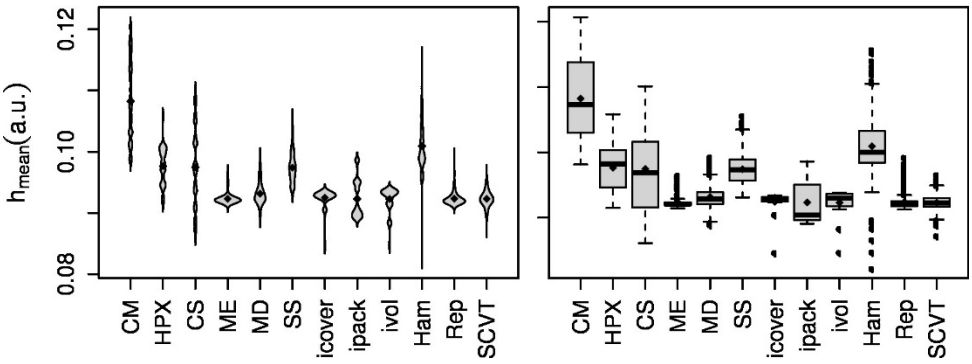

Figure 4. The h_{mean} distributions for the spherical codes with about 580 points, in beanplot (left) and boxplot (right) representation. In the boxplots, the boxes cover the interquartile range and the whiskers extend to the most extreme data point, but not further than 1.5 times the interquartile range [34]. The full knots inside the beans and boxes are the data's mean values and the horizontal lines inside the boxes are the data's median values.

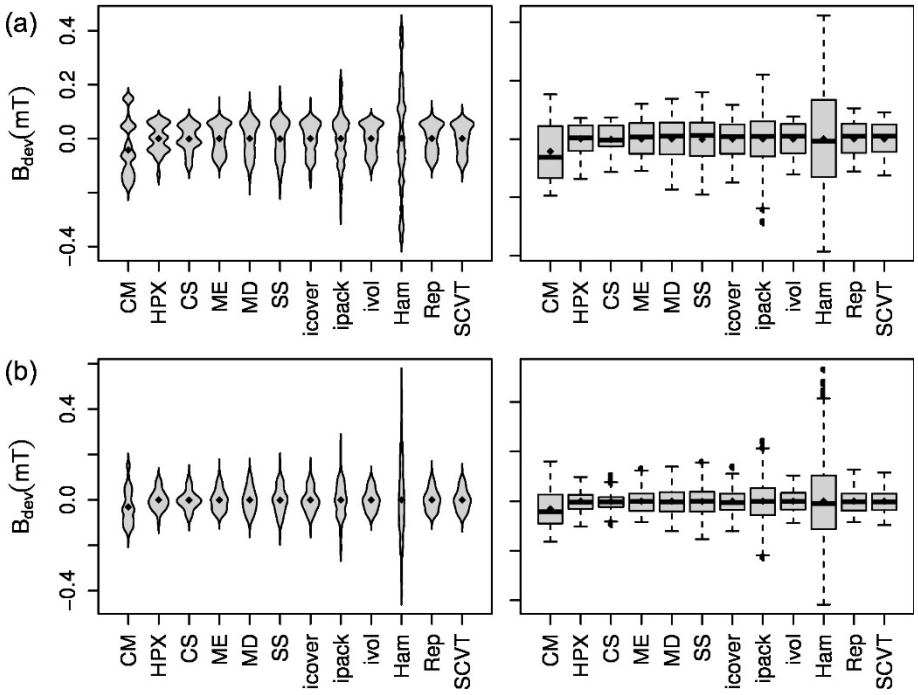

Figure 5. The B_{dev} distributions for the spherical codes with about 580 points, in beanplot (left) and boxplot (right) representation: (a) (C3) g-case, (b) (C4) g-case.

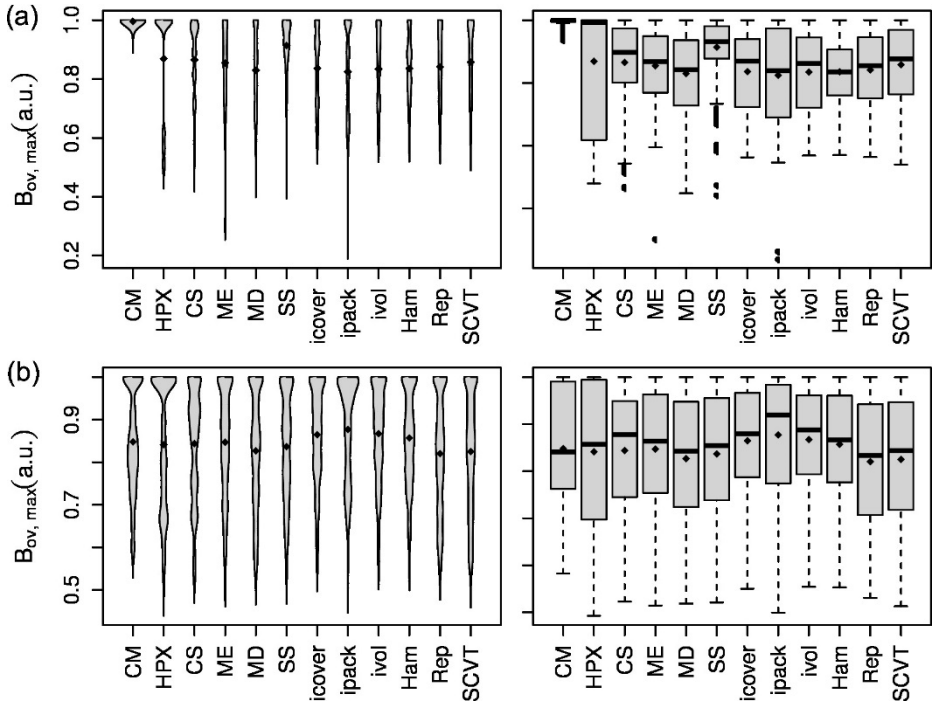

Figure 6. The $B_{ov,max}$ distributions for the spherical codes with about 580 points, in beanplot (left) and boxplot (right) representation: (a) (C3) g-case, (b) (C4) g-case.

Table 1. The mean and median values[1] of the $B_{ov,max}$ distributions, in the axial (C3) and rhombic (C4) g-cases

Grid	(C3)	(C4)
CM	0.996 (1.000)	0.848 (0.840)
HPX	0.869 (0.994)	0.841 (0.855)
CS	0.866 (0.898)	0.844 (0.877)
ME	0.855 (0.869)	0.847 (0.864)
MD	0.830 (0.841)	0.827 (0.842)
SS	0.914 (0.934)	0.836 (0.850)
icover	0.836 (0.867)	0.865 (0.879)
ipack	0.824 (0.840)	0.877 (0.920)
ivol	0.835 (0.859)	0.867 (0.887)
Ham	0.835 (0.837)	0.857 (0.864)
Rep	0.838 (0.852)	0.842 (0.860)
SCVT	0.828 (0.831)	0.839 (0.856)

[1]The median values are given in parentheses. The reported values are the averages on three different sampling experiments of the grids, as described in [4]. Three variants of the Rep and SCVT grids have been used, each sampled once.

CONCLUSIONS

This paper has compared twelve spherical codes regarding their behaviour in CW EPR powder simulations and their homogeneity and EPR properties. The grids' EPR simulations and metrics are only partially consistent. The grids with high geometric and EPR homogeneity do not always generate low-noise simulated EPR spectra. For example, the Repulsion, MD, and SCVT grids generate relatively low-noise simulated EPR spectra and present geometrically and EPR (regarding the B_{dev} metric) homogeneous Voronoi cells. The CM grid, at its turn, generates noisy EPR simulated spectra and has geometrically inhomogeneous and highly EPR-overlapping Voronoi regions. However, the Ham spherical code generates a relatively low-noise simulated EPR spectrum for an axial symmetry spin system, but has geometrically and EPR (B_{dev}) inhomogeneous Voronoi cells.

COMPUTATIONAL DETAILS

The HEALPix spherical code was generated using the `HEALPix` (Hierarchical Equal Area isoLatitude Pixelation of the sphere) software (version 3.30, C language routines) [9]. The Minimum Energy (`me23.0576`) [16], Maximum Determinant (`md023.00576`) [17], and Symmetric Spherical (`ss033.00564`) [18] codes were computed by R. S. Womersley and I. H. Sloan. The Icosahedral arrangements of points (`icover.3.572.7.1.txt`, `ipack.3.582.txt`, and `ivol.3.572.7.1.txt`) were computed by R. H. Hardin, N. J. A. Sloane and W. D. Smith and made available at [19]. The Hammersley spherical code with base 2 was computed with the `udpoint` archive [24]. The Repulsion grids were generated as described in reference [31], using the `repulsion.c` program [25]. The SCVT grids were computed as described in [31], using the FORTRAN90 `sphere_cvt` library (`sphere_cvt.f90`, J. Burkardt) [29]. The Repulsion and SCVT spherical codes were generated in three variants. The Voronoi tessellations of the grids were computed using the `STRIPACK` package (R. J. Renka) [32], in the implementation available at [33] (`stripack.f90`, version 2007).

All CW EPR powder simulations used the microwave frequency v = 9.5 GHz and Gaussian lineshapes with the full width at half maximum of 3 mT. The cubature weight of each grid point to the simulation was approximated with the area of the corresponding Voronoi cell. The homogeneity and EPR metrics were computed as described in reference [4] and the figures were generated within R software environment [34].

REFERENCES

[1]. S. Stoll, Ph.D. Thesis, ETH Zurich, Switzerland, **2003**.
[2]. A. Ponti, *J. Magn. Reson.*, **1999**, *138*, 288.
[3]. M. Bak, N.C. Nielsen, *J. Magn. Reson.*, **1997**, *125*, 132.
[4]. C. Crăciun, *J. Magn. Reson.*, **2014**, *245*, 63.
[5]. H. Nguyen, J. Burkardt, M. Gunzburger, L. Ju, Y. Saka, *Comput. Geom.*, **2009**, *42*, 1.
[6]. P. Shirley, In *Proceedings on Graphics Interface '90*, **1990**, p. 205-212.
[7]. P. Shirley, K. Chiu, *J. of Graphics Tools*, **1997**, *2*, 45.
[8]. K.M. Górski, E. Hivon, A.J. Banday, B.D. Wandelt, F.K. Hansen, M. Reinecke, M. Bartelmann, *The Astrophysical Journal*, **2005**, *622*, 759.
[9]. http://healpix.sourceforge.net
[10]. R. Sadourny, *Mon. Wea. Rev.*, **1972**, *100*, 136.
[11]. C. Ronchi, R. Iacono, P.S. Paolucci, *J. Comput. Phys.*, **1996**, *124*, 93.
[12]. M. Rančić, R.J. Purser, F. Mesinger, *Quart. J. Roy. Meteor. Soc.*, **1996**, *122*, 959.
[13]. R.D. Nair, S.J. Thomas, R.D. Loft, *Mon. Wea. Rev.*, **2005**, *133*, 814.
[14]. R.S. Womersley, I.H. Sloan, *Adv. Comput. Math.*, **2001**, *14*, 195.
[15]. I.H. Sloan, R.S. Womersley, *Adv. Comput. Math.*, **2004**, *21*, 107.
[16]. http://web.maths.unsw.edu.au/~rsw/Sphere/Energy/index.html
[17]. http://web.maths.unsw.edu.au/~rsw/Sphere/Extremal/New/index.html
[18]. http://web.maths.unsw.edu.au/~rsw/Sphere/EffSphDes/ss.html
[19]. R.H. Hardin, N.J.A. Sloane, W.D. Smith, "Tables of spherical codes with icosahedral symmetry", published electronically at http://neilsloane.com/icosahedral.codes/
[20]. J.M. Hammersley, *Ann. New York Acad. Sci.*, **1960**, *86*, 844.
[21]. H. Niederreiter, "Random Number Generation and Quasi-Monte Carlo Methods", *CBMS-NSF Regional Conference Series in Applied Mathematics*, SIAM, Philadelphia, **1992**.
[22]. T.-T. Wong, W.-S. Luk, P.-A. Heng, *J. of Graphics Tools*, **1997**, *2*, 9.
[23]. J. Cui, W. Freeden, *SIAM J. Sci. Comput.*, **1997**, *18*, 595.
[24]. http://www.cse.cuhk.edu.hk/~ttwong/papers/udpoint/udpoints.html
[25]. http://bionmr.chem.au.dk/download/repulsion/repulsion.c
[26]. Q. Du, M.D. Gunzburger, L. Ju, *SIAM J. Sci. Comput.*, **2003**, *24*, 1488.
[27]. Q. Du, M.D. Gunzburger, L. Ju, *Comput. Methods Appl. Mech. Eng.*, **2003**, *192*, 3933.
[28]. J. Burkardt, M. Gunzburger, J. Peterson, R. Brannon, Technical Report: SAND2002-0099, Sandia National Laboratories, February **2002**.
[29]. http://people.sc.fsu.edu/~jburkardt/f_src/sphere_cvt/sphere_cvt.html
[30]. S. Stoll, A. Schweiger, *J. Magn. Reson.*, **2006**, *178*, 42.
[31]. C. Craciun, *Appl. Magn. Reson.*, **2010**, *38*, 279.

[32]. R.J. Renka, *ACM Trans. Math. Softw.*, **1997**, *23*, 416.
[33]. http://people.sc.fsu.edu/~jburkardt/f_src/stripack/stripack.html
[34]. http://www.r-project.org/